Nuclear Physics B325 (1989) 557–580
North-Holland, Amsterdam

ORIENTED $O(\alpha_s^2)$ 3-JET EVENTS IN e^+e^--ANNIHILATION

G.A. SCHULER

Deutsches Elektronen-Synchrotron DESY, D-2000 Hamburg, West Germany

J.G. KÖRNER

Institut für Physik d. Johannes Gutenberg-Universität, Staudinger Weg 7, Postfach 3980, D-6500 Mainz, West Germany
and
Deutsches Elektronen-Synchrotron DESY

Received 30 September 1987
(Revised 30 November 1988)

We present $O(\alpha_s^2)$ expressions for the invariant structure functions that describe the space orientation of $O(\alpha_s^2)$ 3-jet events in e^+e^--annihilation on and off the Z_0. Our results are presented in a form which allows them to be easily incorporated into Monte-Carlo event-generation programs including beam-polarization effects. We present $O(\alpha_s^2)$ thrust distributions for the various helicity cross sections that can be determined from an angular analysis of 3-jet events.

1. Introduction

The measurement of the orientation of 2-jet events in e^+e^--annihilation relative to the beam axis has been of crucial importance in establishing the spin-$\frac{1}{2}$ nature of quark partons [1]. The corresponding measurement of the space orientation of 3-jet events and a comparison with the QCD predictions is also very important for obvious reasons, but has not been attempted so far due to the lack of statistics. Such measurements will be possible in the near future with higher statistics coming from the final analysis of the PETRA data, from PEP, TRISTAN and in particular from SLC and LEP running on the Z_0. The orientation of $O(\alpha_s)$ 3-jet events was studied in the work of Kramer, Schierholz and Willrodt [2]. In particular they calculated the thrust distributions of the various helicity cross sections that characterize the orientation of the 3-jet events. We extend this work by calculating the thrust distributions of the 3-jet helicity cross sections up to $O(\alpha_s^2)$. Present Monte-Carlo 3-jet event-generation programs are incomplete in the sense that the correct $O(\alpha_s^2)$ 3-jet orientation is not yet implemented. They (incorrectly) assign the $O(\alpha_s)$ 3-jet orientation to the $O(\alpha_s^2)$ 3-jet events. This is correct for the leading y-terms ($\ln^2 y + \ln y$ terms), but not correct for the next-to-leading terms (y denotes the

0550-3213/89/$03.50

scaled invariant mass cut-off). It is not clear whether this omission affects the $O(\alpha_s^2)$ analysis of the 3-jet events and thereby the α_s-determination much. However, in view of the fact that a recent analysis has shown that it is difficult to account for the e^+e^- 3-jet and 4-jet data within perturbative QCD [3], one should attempt to eliminate all possible sources of errors that go into such an analysis. One of the purposes of this paper is to provide the necessary $O(\alpha_s^2)$ formulas that allow one to generate $O(\alpha_s^2)$ 3-jet events with the correct orientation including the effects of longitudinal and transverse beam-polarization and parity-violating effects. Concerning the parity-conserving (p.c.) case longitudinal $O(\alpha_s^2)$ 3-jet cross sections have already been published by Kramer and Lampe [4, 5]. In principle these 3 longitudinal cross sections and the total $O(\alpha_s^2)$ cross section calculated in refs. [6, 7] constitute a complete set of 3-jet p.c. cross sections. However, the results of refs. [4, 5] are beset with transcription mistakes including the Erratum on ref. [4] in ref. [5]. Thus we did a complete re-evaluation of the p.c. invariant structure functions and a number of cross checks in order to be able to present correct formulas. The parity-violating (p.v.) invariant structure functions have already been given in [8] and are included here for completeness.

The plan of the paper is as follows. In sect. 2 we briefly sketch the steps and state the definitions that have been used to arrive at our end-results in the later sections in order to provide the appropriate background sources. We are very brief on calculational and technical details since excellent expositions exist on the subject in the literature [6, 7]. In sect. 3 we define the invariant 3-jet cross section in terms of the invariant contraction of a lepton and a hadron tensor. Such a form is suitable for use in the Ali et al. Monte-Carlo event-generation program*. The 3-jet cross section includes the full structure of the standard electroweak model on and off the Z_0. We present explicit formulas for the unpolarized lepton tensor, while longitudinal and transverse beam polarization effects are deferred to appendix A. The hadron tensor is expanded into a standard set of invariant structure functions and their associated covariants. Explicit formulas are then given for the squared matrix element corresponding to the contraction of the lepton and hadron tensors. Sect. 4 contains the QCD dynamics in terms of explicit expressions for the invariant structure functions up to $O(\alpha_s^2)$. In sect. 5 we define helicity cross sections that appear as angular coefficients in the angular distribution of 3-jet events relative to the beam axis. These are related to the standard set of invariant structure functions. One of the set of helicity cross sections (where the quark defines the z-axis and the antiquark lies in the positive (x, z) half plane) is useful for an implementation of the $O(\alpha_s^2)$ effects into the Lund Monte-Carlo event-generation program [10]. Since the Lund MC program has already incorporated the full electro-weak structure and beam polarization effects in terms of the helicity cross sections the inclusion of these effects is automatic if one works with the helicity cross sections. In sect. 5 we also

* The so-called Ali-Monte-Carlo is based on a number of papers. See for some of these ref. [9].

calculate $O(\alpha_s^2)$ thrust distributions of the helicity cross sections in the manner of ref. [2], which contains the $O(\alpha_s)$ results. The $O(\alpha_s^2)$ thrust distribution of the longitudinal cross section corrects the result of ref. [5]. The thrust distributions dH_U/dT (unpolarized transverse), dH_T/dT (transverse–transverse interference) and dH_I/dT (transverse–longitudinal interference) are new. Sect. 6 contains our summary and the conclusions.

In appendix A we write down the full polarization dependence of the 3-jet cross section in an invariant product form appropriate for an implementation in the Ali et al. Monte-Carlo program. In appendix B we write down $O(\alpha_s^2)$ expressions for a set of longitudinal cross sections which have the merit of being very compact. These are related to the helicity cross sections used in the Lund Monte-Carlo program.

2. Some brief technical remarks

The calculation of the $O(\alpha_s^2)$ QCD radiative corrections involves (i) the calculation of loop-graph contributions and (ii) the calculation of the tree-graph contributions integrated over the relevant infrared (IR) and mass (M)* singular regions. We regularize the infinities with dimensional regularization. The relevant details have been described in refs. [6, 7]. IR/M singularities cancel among loop- and tree-graph contributions and the UV singularities are treated within a given subtraction scheme (in our case the $\overline{\text{MS}}$ scheme). Two methods have been used to calculate the loop contributions. In the first method one first does the loop integrations on the amplitude level and then folds these with the relevant Born term amplitudes to obtain the hadron tensor of interest [11]. In the second method one first folds in the relevant Born term amplitudes and then performs the loop integrations [4]. Technically, the latter method is simpler although one looses some of the full spin information contained in the loop amplitudes of the former method. Since the two calculational methods are very different from one another they are useful for cross checking the loop results. We have rechecked the 1-loop expressions of the 4 p.c. invariant structure functions written down by us in ref. [11] which were calculated using the first method. We then converted these to the 4-helicity cross sections H_{U+L}, H_{L1}, H_{L2} and H_{L3} and compared them to the corresponding expressions in refs. [4, 5] calculated by the second method. Discrepancies in the two results were traced to transcription errors in refs. [4, 5] by the authors of refs. [4, 5]. We also did a complete re-evaluation of H_{U+L} using the second method and found agreement with the results of refs. [6, 7]. We are therefore confident that the one-loop results for the p.c. invariant structure functions calculated in ref. [11] and used in this work are correct. The one-loop expressions for the two p.v. invariant structure functions were calculated from the *same* 1-loop amplitudes used to calculate the p.c. structure functions. Since these were checked against an independent calculation in the p.c.

* We work with mass-zero quarks.

case we are also confident that the p.v. 1-loop results written down in ref. [11], used in ref. [8] and in this work are correct*. Concerning the tree-graph contributions we re-calculated the four p.c. helicity cross sections H_{U+L}, H_{L1}, H_{L2} and H_{L3}, which were also calculated in ref. [5]. The two p.v. tree-graph structure functions were calculated in ref. [8]. The tree-graph IR/M integration regions are defined via an invariant mass cut-off $y \leqslant (p_i + p_j)^2/q^2$ $(i \neq j = 1, \ldots, 4)$. If *any* of the 6 invariant masses $s_{ij} = (p_i + p_j)^2$ is smaller than yq^2 the event is called a 3-jet event. The integrations within this IR/M region were then done up to $O(y^0)$ accuracy, i.e. we included $\ln y$, $\ln^2 y$ and constant terms in our result**. In the $O(y^0)$ approximation the tree-graph contributions have a rather simple structure: one has an universal IR/M factor which multiplies the Born term structure [5, 8]. We have checked that the integrand that leads to the universal IR/M factor after IR/M integration is identical to the corresponding integrand in the tree-graph calculation of the trace of the hadronic tensor in ref. [7]. It is also important to state that the overlapping singularities occurring in the tree-graph integrand have been integrated using the "direct-dressing approach" of ref. [5] (see also ref. [12]), i.e. they have been integrated in the domain where for *any* pair of momenta $(p_i + p_j)^2 \leqslant yq^2$ $(i \neq j)$ without partial fractioning of the overlapping divergencies. It is well-known that the "partial fractioning approach" differs from the direct-dressing approach by finite term contributions [12]. The two approaches differ by apportioning finite term contributions differently to the $O(\alpha_s^2)$ 3-jet and 4-jet domain [12]. The appropriate 4-jet Monte Carlo that continuously fits on to our 3-jet definition is the usual one where the 4-jet domain is defined by $(p_i + p_j)^2 \geqslant yq^2$ for *all* p_i and p_j $(i \neq j)$.

3. Lorentz invariant cross sections

For unpolarized beams the 3-parton cross section $e^+(q_+)e^-(q_-) \to q(p_1)\bar{q}(p_2)g(p_3)$ is given by (see e.g. ref. [13])

$$d\sigma = (2\pi\alpha/q^2)^2 \left[g_{11}(Q_f) L^{(1)}_{\mu\nu} H^{\mu\nu}_{(1)} + g_{44}(Q_f) L^{(4)}_{\mu\nu} H^{\mu\nu}_{(4)} \right] d\,\mathrm{LIPS}^{(3)}. \tag{3.1}$$

The polarized-beam cross section is treated in appendix A.

The Lorentz-invariant phase space in eq. (3.1) reads

$$d\mathrm{LIPS}^{(3)} = (2\pi)^4 \delta(p_1 + p_2 + p_3 - q) \frac{d^3p_1}{(2\pi)^3 2E_1} \frac{d^3p_2}{(2\pi)^3 2E_2} \frac{d^3p_3}{(2\pi)^3 2E_3}. \tag{3.2}$$

* Some printing errors in ref. [11] containing the p.v. case have been corrected in an Erratum [8].

** For the present discussion we assume that the invariant mass cut y is always chosen small enough so that the IR/M integration region is determined by the nominal y-cut and *not* by 4-body kinematics close to the 2-jet limit. See ref. [12] and the discussion in sect. 5.

The weak-isospin-dependent coupling coefficients $g_{11}(Q_f)$ and $g_{44}(Q_f)$ specify the electroweak-model dependence. In the standard Weinberg–Salam model one has for

$\underline{Q_f = \frac{2}{3}(u, c, t)}$

$$g_{11} = \tfrac{4}{9} - \tfrac{4}{3}\left(-1 + 4\sin^2\Theta_W\right)\left(1 - \tfrac{8}{3}\sin^2\Theta_W\right)\mathrm{Re}\,\chi_Z + \left[\left(-1 + 4\sin^2\Theta_W\right)^2 + 1\right]\left[\left(1 - \tfrac{8}{3}\sin^2\Theta_W\right) + 1\right]|\chi_Z|^2$$

$$g_{44} = \tfrac{4}{3}\mathrm{Re}\,\chi_Z - 4\left(-1 + 4\sin^2\Theta_W\right)\left(1 - \tfrac{8}{3}\sin^2\Theta_W\right)|\chi_Z|^2 \qquad (3.3)$$

$\underline{Q_f = -\frac{1}{3}(d, s, b)}$

$$g_{11} = \tfrac{1}{9} + \tfrac{2}{3}\left(-1 + 4\sin^2\Theta_W\right)\left(-1 + \tfrac{4}{3}\sin^2\Theta_W\right)\mathrm{Re}\,\chi_Z + \left[\left(-1 + 4\sin^2\Theta_W\right)^2 + 1\right]\left[\left(-1 + \tfrac{4}{3}\sin^2\Theta_W\right)^2 + 1\right]|\chi_Z|^2$$

$$g_{44} = \tfrac{2}{3}\mathrm{Re}\,\chi_Z + 4\left(-1 + 4\sin^2\Theta_W\right)\left(-1 + \tfrac{4}{3}\sin^2\Theta_W\right)|\chi_Z|^2, \qquad (3.4)$$

where

$$\chi_Z = \frac{gM_Z^2 q^2}{q^2 - M_Z^2 + iM_Z\Gamma_Z}, \qquad g = \frac{G_F}{8\sqrt{2}\pi\alpha} \approx 4.49 \times 10^{-5}\ \mathrm{GeV}^{-2}. \qquad (3.5, 3.6)$$

The parity-conserving lepton tensor $L_{\mu\nu}^{(1)}$ and the parity-violating lepton tensor $L_{\mu\nu}^{(4)}$ are given by

$$L_{\mu\nu}^{(1)} = (2/q^2)\left(q_{+\mu}q_{-\nu} + q_{-\mu}q_{+\nu} - \tfrac{1}{2}q^2 g_{\mu\nu}\right)$$

$$L_{\mu\nu}^{(4)} = \left(-2i/q^2\right)\varepsilon_{\mu\nu\alpha\beta}q_+^\alpha q_-^\beta, \quad (\varepsilon_{0123} = +1). \qquad (3.7)$$

The p.c. hadron tensor $H_{\mu\nu}^{(1)}$ and the p.v. hadron tensor $H_{\mu\nu}^{(4)}$ are defined by

$$H_{\mu\nu}^{(1)} = \sum_{\text{spins}} \left\langle q\bar{q}g\middle| j_\mu{}^V\middle|0\right\rangle \left\langle q\bar{q}g\middle| j_\nu{}^V\middle|0\right\rangle^*,$$

$$H_{\mu\nu}^{(4)} = \sum_{\text{spins}} \left\langle q\bar{q}g\middle| j_\mu{}^V\middle|0\right\rangle \left\langle q\bar{q}g\middle| J_\nu^A\middle|0\right\rangle^*. \qquad (3.8)$$

We shall present our $O(\alpha_s)$ and $O(\alpha_s^2)$ QCD results in sect. 4 using a standard set of hadron tensor invariants defined by the covariant expansion

$$H_{\mu\nu}^{(1)} = \left(g_{\mu\nu} - \frac{q_\mu q_\nu}{q^2}\right) H_1 + (1/q^2)\hat{p}_{1\mu}\hat{p}_{1\nu} H_2$$

$$+ (1/q^2)\hat{p}_{2\mu}\hat{p}_{2\nu} H_3 + (1/q^2)(\hat{p}_{1\mu}\hat{p}_{2\mu} + \hat{p}_{1\nu}\hat{p}_{2\mu}) H_4, \tag{3.9}$$

$$H_{\mu\nu}^{(4)} = (1/q^2) i\varepsilon_{\mu\nu\alpha\beta} q^\alpha (p_1^\beta H_6 + p_2^\beta H_7), \tag{3.10}$$

where $\hat{p}_{i\mu} = p_{i\mu} - (p_i q/q^2) q_\mu$. In the most general 3-particle final state case there are one more p.c. invariant H_5 (multiplying the covariant $\hat{p}_{1\mu}\hat{p}_{2\nu} - \hat{p}_{1\nu}\hat{p}_{2\mu}$) and two more p.v. invariants H_8 and H_9 (multiplying the covariants $(\hat{p}_{i\mu}\varepsilon_{\nu\alpha\beta\gamma} p_1^\alpha p_2^\beta p_3^\gamma + \mu \leftrightarrow \nu)$, $i = 1, 2$) in the general expansion (3.9) and (3.10). Their contributions are determined by the imaginary parts of the hadron tensor $H_{\mu\nu}$. These can be shown to vanish in massless QCD at $O(\alpha_s^2)$ [11, 14]. It is now straightforward to evaluate the lepton–hadron contractions $L_{\mu\nu} H^{\mu\nu}$ occurring in eq. (3.1). One has

p.c. case:

$$L_{\mu\nu}^{(1)} H_{(1)}^{\mu\nu} = -2H_1 + (4/q^4)(p_1 q_+)(p_1 q_-) H_2 + (4/q^4)(p_2 q_+)(p_2 q_-) H_3$$

$$+ (4/q^4)[(p_1 q_-)(p_2 q_-) + (p_1 q_-)(p_2 q_+)] H_4, \tag{3.11}$$

p.v. case:

$$L_{\mu\nu}^{(4)} H_{(4)}^{\mu\nu} = -(2/q^2)[p_1(q_- - q_+)] H_6 - (2/q^2)[p_2(q_- - q_+)] H_7. \tag{3.12}$$

4. Invariant structure functions up to $O(\alpha_s^2)$

As described in sect. 2 one obtains the invariant structure functions from the sum of 1-loop and tree-graph contributions. IR/M singularities cancel among the two contributions and the remaining UV singularities are subtracted using the $\overline{\text{MS}}$ renormalization scheme. One has ($C_F = \frac{4}{3}$, $N_C = 3$, N_f = number of flavours)

p.c. case

$i = 1, 2, 3$:

$$H_i = 32\pi^2 C_F N_C B_i \frac{a_s}{2\pi}\left\{1 + \frac{\alpha_s}{2\pi}\left[\tfrac{1}{2}N_C\left(\tilde{H}(\text{tree}) + \frac{1}{B_i}\tilde{H}_i(\text{loop})\right)\right.\right.$$

$$\left.\left. + (C_F - \tfrac{1}{2}N_C)\left(\hat{H}(\text{tree}) + \frac{1}{B_i}\hat{H}_i(\text{loop})\right) + (\tfrac{1}{3}N_f - \tfrac{11}{6}N_C) H^f(\text{tree})\right]\right\}, \tag{4.1}$$

where the B_i denote the Born term functions

$$B_1 = -\frac{x_1^2 + x_2^2}{(1-x_1)(1-x_2)}, \qquad B_2 = B_3 = -\frac{4}{(1-x_1)(1-x_2)}, \quad (4.2, 4.3)$$

and where the remainders of the universal "IR/M" factors (after removal of the singular pieces) are given by

$$\tilde{H}(\text{tree}) = \tfrac{25}{3} + \tfrac{2}{3}\pi^2 - \ln^2 y_{13} - \ln^2 y_{23} - 4\ln^2 y - 3\ln y + 4\ln y \ln(y_{13}y_{23}),$$

$$\hat{H}(\text{tree}) = 7 + \tfrac{1}{3}\pi^2 - \ln y_{12} - 2\ln^2 y - 3\ln y + 4\ln y \ln y_{12},$$

$$H^{\text{f}}(\text{tree}) = -\tfrac{5}{3} + \ln y. \qquad (4.4)$$

We have used the usual scaled energy variables x_i with $2p_iq = x_iq^2$ and $2p_ip_j = y_{ij}q^2 = (1-x_k)q^2 \quad (k \neq i, j)$.

For H_4 there is no $O(\alpha_s)$ contribution and consequently also no $O(\alpha_s^2)$ "tree" contribution in the $O(y^0)$ approximation. One has

$$H_4 = 32\pi^2 C_F N_C \left(\frac{\alpha_s}{2\pi}\right)^2 \left[\tfrac{1}{2}N_C \tilde{H}_4(\text{loop}) + \left(C_F - \tfrac{1}{2}N_C\right)\hat{H}_4(\text{loop})\right]. \qquad (4.5)$$

The "loop" contributions $\tilde{H}_i(\text{loop})$ and $\hat{H}_i(\text{loop})$ are listed in tables 1 and 2. Note that the classification in terms of (tree) and (loop) contributions is somewhat arbitrary in that the finite contributions can be re-distributed among the two. In

TABLE 1

QCD loop contributions to 4 p.c. structure functions H_i. Entries denoted by ← s are obtained from their left neighbours by interchanging 1 and 2. Entries denoted by ↑ s are obtained from their upper neighbours by interchanging 1 and 2. The scaled energy variables x_i and y_{ij} are defined after eq. (4.4).

QCD		$\ln y_{23}$	$\ln y_{13}$	$r(y_{13}, y_{23})$
$\tilde{H}_1$	$-7 \cdot B_1 + \dfrac{(1-x_3)(x_1+x_2)}{(1-x_1)(1-x_2)}$	$-3\dfrac{x_2}{x_1} - \ln y_{23} B_1$	← s	$-2B_1$
$\tilde{H}_2$	$-7 \cdot B_2 + \dfrac{2x_2(x_1+x_2)}{x_1(1-x_1)(1-x_2)}$	$\dfrac{2x_2^2}{x_1^2(1-x_1)(1-x_2)} - \ln y_{23} B_2$	$\dfrac{-6}{(1-x_1)(1-x_2)} - \ln y_{13} B_2$	$-2B_2$
$\tilde{H}_3$	↑ s	$\dfrac{-6}{(1-x_1)(1-x_2)} - \ln y_{23} B_2$	$\dfrac{2x_1^2}{x_2^2(1-x_1)(1-x_2)} - \ln y_{13} B_2$	↑ s
$\tilde{H}_4$	$-2\dfrac{x_1+x_2}{x_1x_2}$	$-2\dfrac{(1-x_1)(1-x_2)+x_1x_2}{x_1^2(1-x_1)(1-x_2)}$	← s	0

TABLE 2
QED loop contributions to 4 p.c. structure functions H_i. Notation $\leftarrow$ ($\uparrow$)s as in table 1. $X = (1-x_1)(1-x_2)(1-x_3)$.

QED		$\ln y_{12}$
$\hat{H}_1$	$-7\cdot B_1$ $+\dfrac{(x_1-x_2)^2+x_1+x_2}{(1-x_1)(1-x_2)}$	$-B_1\cdot\ln y_{12}$ $+\dfrac{2(1-x_3)(x_1+x_2-2x_1x_2)}{x_3(1-x_1)(1-x_2)}$
$\hat{H}_2$	$-7\cdot B_2$ $+2\dfrac{4x_1(1-x_2(1-x_2))+x_2x_3(x_1+x_2)}{x_1x_3(1-x_1)(1-x_2)}$	$-B_2\cdot\ln y_{12}$ $+4\dfrac{x_2^2x_3^2-2x_1x_2(1-x_1)(1-x_2)+2(1+x_2)X}{x_3^2(1-x_1)^2(1-x_2)^2}$
$\hat{H}_3$	$\uparrow$s	$\uparrow$s
$\hat{H}_4$	$-\{x_1x_2x_3(x_3-6(1-x_3))-8x_1x_2(x_1^2+x_2^2)$ $+x_1x_3(x_3^2-x_1^2)+x_2x_3(x_3^2-x_2^2)\}\cdot$ $\dfrac{1}{2x_1x_2x_3(1-x_1)(1-x_2)}$	$4\dfrac{x_3^2(1-x_3)+(1-x_1)(1-x_2)(x_1^2+x_2^2-x_3)}{x_3^2(1-x_1)^2(1-x_2)^2}$

QED	$\ln y_{13}$	$\ln y_{23}$	$r(y_{12},y_{13})$	$r(y_{12},y_{23})$
$\hat{H}_1$	$\dfrac{x_1(1+x_1-2x_3)}{x_2(1-x_1)}$	$\leftarrow$s	$2\dfrac{x_2^2(1-x_1)+x_1x_3(1-x_3)}{(1-x_1)^2(1-x_2)}$	$\leftarrow$s
$\hat{H}_2$	$2\dfrac{1+x_1-2x_3}{(1-x_1)^2(1-x_2)}$	$\dfrac{2x_2^2(2x_1+1-x_2)}{x_1^2(1-x_1)(1-x_2)^2}$	$4\dfrac{(1-x_3)^2+(1-x_1)^2}{(1-x_1)^3(1-x_2)}$	$4\dfrac{x_2^2+2(1-x_2)^2}{(1-x_1)(1-x_2)^3}$
$\hat{H}_3$	$\dfrac{2x_1^2(2x_2+1-x_1)}{x_2^2(1-x_1)^2(1-x_2)}$	$2\dfrac{1+x_2-2x_3}{(1-x_1)(1-x_2)^2}$	$4\dfrac{x_1^2+2(1-x_1)^2}{(1-x_1)^3(1-x_2)}$	$4\dfrac{(1-x_3)^2+(1-x_2)^2}{(1-x_1)(1-x_2)^3}$
$\hat{H}_4$	$2\dfrac{(1-x_3)^2+(1-x_3)\cdot x_2-2(1-x_1)^2(1-x_2)}{2(1-x_1)^2(1-x_2)}$	$\leftarrow$s	$4\dfrac{x_1^2+x_2-1}{(1-x_1)^3(1-x_2)}$	$\leftarrow$s

exception are the y-dependent terms which truly come from the tree-graph contributions. Following the terminology of ref. [4] the "tilde $\sim$" contributions denote QCD-type contributions and the "hat $\hat{}$" contributions denote QED-type contributions.

p.v. case

$$H_6 = 32\pi^2 C_F N_C B_6(\alpha_s/2\pi)\Big\{1 + \frac{\alpha_s}{2\pi}\Big[\tfrac{1}{2}N_C\big(\tilde{H}(\text{tree}) + (1/B_6)\tilde{H}_6(\text{loop})\big)$$

$$\times\big(C_F - \tfrac{1}{2}N_C\big)\Big(\hat{H}(\text{tree}) + \frac{1}{B_6}\hat{H}_6(\text{loop}) + \big(\tfrac{1}{3}N_f - \tfrac{11}{6}N_C\big)H^f(\text{tree})\Big)\Big]\Big\} \tag{4.6}$$

$$H_7(1,2) = -H_6(2,1) \tag{4.7}$$

and the Born term function is given by

$$B_6 = \frac{2x_1}{(1-x_1)(1-x_2)}\,. \tag{4.8}$$

The H(tree) appearing in eq. (4.6) are the same universal "IR/M" factors as given in eq. (4.4). The loop contributions are given by

$$\tilde{H}_6(\text{loop}) = B_6\big[7 + \ln^2 y_{13} + \ln^2 y_{23} + 2r(y_{13}, y_{23})\big] + \frac{(1-x_3)(2-x_3)}{x_1(1-x_1)(1-x_2)}$$

$$-\ln y_{13}\frac{5x_1x_2 - 3(1-x_3)}{x_2(1-x_1)(1-x_2)} + \ln y_{23}\frac{x_2(x_1x_2 + 1 - x_3)}{x_1^2(1-x_1)(1-x_2)} \tag{4.9}$$

$$\hat{H}_6(\text{loop}) = -\big(9 + \ln^2 y_{12}\big)B_6$$

$$+\frac{x_3^2(1-x_3) + 2(1-x_1)[x_1(x_1+x_2) - x_3(1-x_3)]}{x_1x_3(1-x_1)(1-x_2)}$$

$$+2\ln y_{12}\frac{x_2(1-x_3) + x_3 - x_1}{x_3^2(1-x_1)(1-x_2)} + \ln y_{13}\frac{3(1-x_1)(1-x_2) + 2x_2(1-x_3)}{x_2(1-x_1)(1-x_2)}$$

$$+\ln_{23}\frac{(1-x_1)(1-x_2)(x_3-x_1) - 2(1-x_3)^2}{x_1^2(1-x_1)(1-x_2)}$$

$$+2r(y_{12}, y_{13})\frac{(1-x_3)(x_1-x_3)}{(1-x_1)^2(1-x_2)} - 2r(y_{12}, y_{23})\frac{2x_1(1-x_2) + x_2(1-x_3)}{(1-x_1)(1-x_2)^2}\,, \tag{4.10}$$

where

$$r(x, y) = \ln x \ln y - \ln x \ln(1-x) - \ln y \ln(1-y) - L_2(x) - L_2(y) + \tfrac{1}{6}\pi^2 \tag{4.11}$$

and where $L_2(x)$ is the Spence function defined by

$$L_2(x) = -\int_0^x \mathrm{d}z \, \frac{\ln(1-z)}{z} \tag{4.12}$$

5. Thrust distributions of helicity cross sections

For the presentation of experimental results and their comparison with QCD predictions it is convenient to write down the cross section in the e^+e^- c.m. frame in a noncovariant frame-dependent way. One chooses a hadronic reference frame whose orientation relative to the beam ($\hat{=}$ laboratory) frame is specified by three Euler angles Θ, χ and φ. In the case where there is no beam polarization the cross section does not depend on the third (azimuthal) Euler angle φ. In this case one has (see e.g. ref. [13])*

$$\begin{aligned}\frac{\mathrm{d}\sigma}{\mathrm{d}\cos\Theta \, \mathrm{d}\chi \, \mathrm{d}x_1 \, \mathrm{d}x_2} = \frac{1}{64\pi^2} \frac{4\pi\alpha^2}{3q^2} \Big\{ & g_{11}(Q_f)\big[\tfrac{3}{8}(1+\cos^2\Theta) H_U \\ & + \tfrac{3}{4}\sin^2\Theta \, H_L + \tfrac{3}{4}\sin^2\Theta \cos 2\chi \, H_T - (3/2\sqrt{2})\sin 2\Theta \cos\chi \, H_I\big] \\ & + g_{44}(Q_f)\big[\tfrac{3}{4}\cos\Theta \, H_P - (3/\sqrt{2})\sin\Theta \cos\chi \, H_A\big]\Big\} .\end{aligned} \tag{5.1}$$

The x_i are the scaled parton energies in the c.m. frame $2p_iq = x_iq^2$. For the definition of the Euler angles Θ and χ we refer to refs. [13,15]**. These references also contain complete beam-polarization formulas. The helicity cross sections appearing in eq. (5.1) are defined by linear combinations of the helicity components of

* Possible angular dependencies proportional to $\sin\Theta \sin\chi$, $\sin^2\Theta \sin 2\chi$ and $\sin 2\Theta \sin\chi$ are not included, because of the aforementioned vanishing of the contributions of the imaginary parts of the 1-loop contributions for mass-zero quarks.

** Note that refs. [10,15] have a different convention for χ. The relation is $\chi \to \pi - \chi$.

the hadron tensor in a given hadronic reference frame. They are

(i) p.c. case

$$H_U = H_{++} + H_{--} = H_{11} + H_{22}$$
$$H_L = H_{00} = H_{33}$$
$$H_T = \mathrm{Re}\, H_{+-} = \tfrac{1}{2}(-H_{11} + H_{22})$$
$$H_I = \tfrac{1}{2}\mathrm{Re}(H_{+0} - H_{-0}) = (-1/2\sqrt{2})(H_{31} + H_{13}), \tag{5.2}$$

(ii) p.v. case

$$H_P = H_{++} - H_{--} = -i(H_{12} - H_{21})$$
$$H_A = \tfrac{1}{2}\mathrm{Re}(H_{+0} + H_{-0}) = \frac{-i}{2\sqrt{2}}(H_{23} - H_{32}), \tag{5.3}$$

where $H_{mn} = \varepsilon^{\mu}(m) H_{\mu\nu} \varepsilon^{*\nu}(n)$, $\varepsilon_\mu(0) = (0; 0, 0, 1)$ and $\varepsilon_\mu(\pm) = (1/\sqrt{2})(0; \mp 1, -\mathrm{i}, 0)$. Let us mention again that in massless QCD the above six helicity cross section suffice to specify the orientation of 3-jets up to $O(\alpha_s^2)$ even in the presence of beam polarization [11,14]. We shall present our numerical results in terms of the thrust distribution [16]. The thrust of a 3-jet event is determined by the scaled energy x_i of the most energetic jet. The most energetic jet also defines the thrust axis. We discuss the thrust distributions of the four p.c. helicity cross sections in eq. (5.1) in the manner of ref. [2] which contains the $O(\alpha_s)$ results. $O(\alpha_s^2)$ thrust distributions of the p.v. helicity cross sections H_P and H_A have already been discussed in ref. [8] and will not be presented again in this work. We shall specify the hadronic system such that the thrust axis (most energetic parton) is the z-axis and the second most energetic parton determines the positive x-axis*. Such hadronic frame specification has the advantage of requiring no flavour identification. We need, however, to introduce the six helicity frames (i, j) $(i, j = 1, 2, 3)$ where the z-axis is along parton i and parton j lies in the positive (z, x) half plane. Next, we need to relate the helicity cross sections to the invariant structure functions in each of the six helicity frames. For the (1, 2) helicity frame (Lund system) one obtains

$$H_{U1} = -2H_1 + \frac{X}{x_1^2} H_3,$$
$$H_{L1} = -H_1 + \tfrac{1}{4} x_1^2 H_2 + \tfrac{1}{4}\left(\frac{Z_3}{x_1}\right)^2 H_3 + \tfrac{1}{2} Z_3 H_4,$$
$$H_{T1} = -\tfrac{1}{2}\frac{X}{x_1^2} H_3,$$
$$H_{I12} = -\frac{1}{2\sqrt{2}}\sqrt{X}\,\frac{Z_3}{x_1^2} H_3 - \frac{1}{2\sqrt{2}}\sqrt{X}\, H_4, \tag{5.4}$$

* Hadronic event frames with the 3-axis in the event plane are referred to as helicity frames.

where

$$Z_k = x_i x_j \cos\Theta_{ij} = (1-x_i)(1-x_j) - (1-x_k),$$

$$2\sqrt{X} = x_i x_j \sin\Theta_{ij} = 2\sqrt{(1-x_1)(1-x_2)(1-x_3)} \tag{5.5}$$

and Θ_{ij} is the angle between parton i and j. The corresponding expression for the (1,3) helicity frame is obtained from eq. (5.4) by $\sqrt{X} \to -\sqrt{X}$, i.e. $\sigma_{\mathrm{I}} \to -\sigma_{\mathrm{I}}$. The frame dependence of the helicity cross section has been annotated by adding the 3-axis as an index. H_{I} requires specification also of the x-axis. In our notation $H_{\mathrm{I}13} = -H_{\mathrm{I}12}$. The corresponding relations for the (2,1) and (2,3) helicity frames are obtained from those of the (1,2) and (1,3) helicity frames by $1 \to 2$ exchange which also implies the exchange of H_2 and H_3.

For the (3,1) helicity frame we obtain

$$x_3^2 H_{\mathrm{U}3} = -2x_3^2 H_1 + X(H_2 + H_3 - 2H_4),$$

$$x_3^2 H_{\mathrm{L}3} = -x_3^2 H_1 + \tfrac{1}{4}Z_2^2 H_2 + \tfrac{1}{4}Z_1^2 H_3 + \tfrac{1}{2}Z_1 Z_2 H_4,$$

$$2x_3^2 H_{\mathrm{T}3} = X(-H_2 - H_3 + 2H_4),$$

$$2\sqrt{2}\, x_3^2 H_{\mathrm{I}31} = \sqrt{X}\left(-Z_2 H_2 + Z_1 H_3 - (x_1^2 - x_2^2) H_4\right). \tag{5.6}$$

The corresponding expressions for the (3,2) system are obtained from (5.6) by $\sqrt{X} \to -\sqrt{X}$ ★. We are now in a position to present and discuss the thrust distributions of the various helicity cross sections. In the $O(\alpha_s)$ case the necessary energy integration can be done analytically [2] whereas the complexity of the $O(\alpha_s^2)$ expressions requires a numerical integration. The numerical results depend of course on the choice of the IR/M resolution parameter which is the invariant mass cut parameter y in our case. We shall present curves for the two choices $y = 0.01$ and $y = 0.04$. The smaller value $y = 0.01$ is a better choice since it minimizes two sources of errors that have been incurred in the QCD calculations leading to the analytical results in sect. 4. The first error is of $O(y)$ and derives from the accuracy with which the IR/M tree-graph integrations have been done. The second error is kinematical in nature and is of $O(\ln(y_{ij}/y))$ in those regions of phase space close to the 2-jet region where the IR/M region is not bounded by the nominal invariant mass cut y, but by the kinematic boundary characterized by some invariant mass $y_{ij} < y$. These are the regions of phase space with high thrust values: high thrust values can be

★ In the Lund MC one also needs to evaluate the two p.v. helicity cross sections H_{P} and H_{A} in terms of the invariant structure functions H_6 and H_7 in the (1,2) system. The relations are

$$x_1 H_{\mathrm{P}1} = x_1^2 H_6 + Z_3 H_7, \qquad \sqrt{2}\, x_1 H_{\mathrm{A}12} = \sqrt{X} H_7.$$

realized by partons only if energy goes into forward motion and not into invariant mass. Since this second source of errors can become quite important for higher thrust values and since this source of errors is not widely appreciated in the literature we have to take a deeper look at the 4-parton kinematics in order to determine the range of validity of our approximate tree-graph evaluations. The IR/M integrations on the tree-graph contributions have been done in the respective c.m. systems of the unresolved parton pairs. For definiteness we choose the $(\boldsymbol{p}_1, \boldsymbol{p}_3)$ c.m. system. Let β be the polar angle of parton 4 relative to parton 2. One has the kinematical relation [7]:

$$\tfrac{1}{2}(1-\cos\beta) = \frac{y_{13}y_{24}}{y_{134}y_{123} - y_{13}(1-y_{24})}, \tag{5.7}$$

where $y_{ijk} = y_{ij} + y_{ik} + y_{jk}$. The kinematical requirement $\cos\beta \geqslant -1$ translates into

$$y_{134}y_{123} \geqslant y_{13}. \tag{5.8}$$

Similar kinematical conditions hold for the other c.m. systems corresponding to the other 5 unresolved parton pairs. Using 3-parton variables these kinematic conditions translate into

$$(1-x_i)(1-x_j) \geqslant y, \qquad i \neq j = 1,2,3, \tag{5.9}$$

where we have now substituted the nominal invariant mass cut y for the respective parton-pair invariant masses. In fig. 1 we have plotted the 3-parton phase space together with the boundary curves (5.9) for $y = 0.01$ and $y = 0.04$. We have also

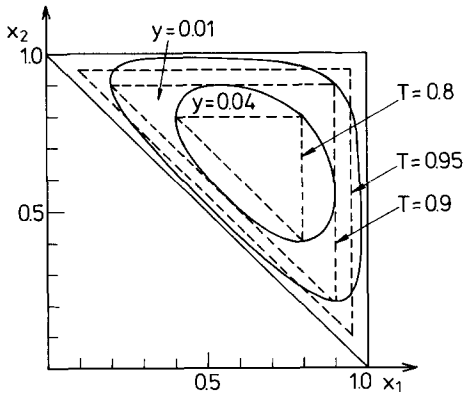

Fig. 1. 3-parton phase space. Full lines: Boundary curves of regions where invariant mass integrations on unresolved parton pairs in the 4-parton case are determined by nominal invariant mass cuts $y = 0.01$ and $y = 0.04$. Dashed lines: Lines of constant thrust $T = 0.8$, 0.9 and 0.95.

drawn lines corresponding to the thrust values $T = 0.8$, 0.9 and 0.95. One can easily convince oneself that the kinematic constraint (5.9) is satisfied for thrust values

$$T \leqslant 1 - \sqrt{y} \,. \tag{5.10}$$

This implies that the second source of errors deriving from 4-parton kinematics close to the 2-jet limit sets in for $T \geqslant 0.9$ and $T \geqslant 0.8$ for $y = 0.01$ and $y = 0.04$, respectively. Only a detailed MC study can reveal how large this thrust dependent error becomes for large thrust values. The calculations of ref. [12] indicate that these errors can become rather large ($\gtrsim 30\%$) for thrust values $T \geqslant 0.95$.

After this long but necessary detour we now proceed to present our results for the thrust distributions of the helicity cross sections H_{U+L}, H_U, H_L, H_T and H_I. In figs. 2a–2e we have drawn the $O(\alpha_s)$ thrust distributions along with the $O(\alpha_s^2)$ curves for the two cut-off values $y = 0.04$ and $y = 0.01$. We have chosen to normalize the helicity cross sections to a normalization factor N which includes the total cross-section ratio calculated to $O(\alpha_s^2)$ in the $\overline{\text{MS}}$ scheme. We take

$$N = 192\pi^2\left[1 + (\alpha_s/\pi) + (1.986 - 0.115\, N_f)(\alpha_s/\pi)^2\right] \tag{5.11}$$

with $N_f = 5$ and $\alpha_s = 0.18$. Depending on the choice of the jet-resolution parameter y the $O(\alpha_s)$ results are changed upward and downward for $y = 0.04$ and $y = 0.01$ over most of the thrust range. The percentage changes of the cross-section values $[H_A(\alpha_s^2) - H_A(\alpha_s)]/H_A(\alpha_s)$ ($A = U + L$, U, L, T, I), for the above cut-off values are plotted in fig. 3. For $y = 0.04$ the biggest percentage change occurs for H_I over most of the thrust range, followed by H_U, H_{U+L}, H_T and H_L in that order. For $y = 0.01$ this order in the percentage changes is reversed. This implies that those parts of the $O(\alpha_s^2)$ corrections that are independent of y are positive and their relative contributions are largest for H_I, followed by H_U, H_{U+L}, H_T and H_L in that order. A comparison of fig. 2c (H_L) and 2d (H_T) shows that the $O(\alpha_s)$ result $2H_T = H_L$ is not changed very much at the $O(\alpha_s^2)$ level. This was investigated in more detail in ref. [16] where the $O(\alpha_s^2)$ corrections to the $O(\alpha_s)$ relation $2H_T = H_L$ were calculated and found to be very small (of $O(1^0/00)$). In particular, this implies that the polar-angle distribution of the normal to the 3-jet plane is $1 - \frac{1}{3}\cos^2\overline{\Theta}$ to a very high level of accuracy ($O(1^0/00)$) even at the $O(\alpha_s^2)$ level ($\overline{\Theta}$ is the polar angle of the normal of the 3-jet plane w.r.t.: the beam axis) as explicitly calculated in ref. [17]. In fig. 4 we present our $O(\alpha_s^2)$ results for the polar asymmetry parameter $\alpha(T) \cdot \alpha(T)$ determines the polar-angle dependence of the cross section, i.e. $\sigma(\Theta) \propto 1 + \alpha(T)\cos^2\Theta$, where Θ is the polar angle of the thrust axis relative to the beam axis. For $y = 0.01$ the $O(\alpha_s^2)$ result is not very different from the $O(\alpha_s)$ curve, whereas for $y = 0.04$ the asymmetry is corrected upwards by more than 10% over a significant range of thrust values. It is clear from what was said above that the $O(\alpha_s^2)$ curves should not be trusted much beyond thrust values $T > 0.9 - 0.95$ for

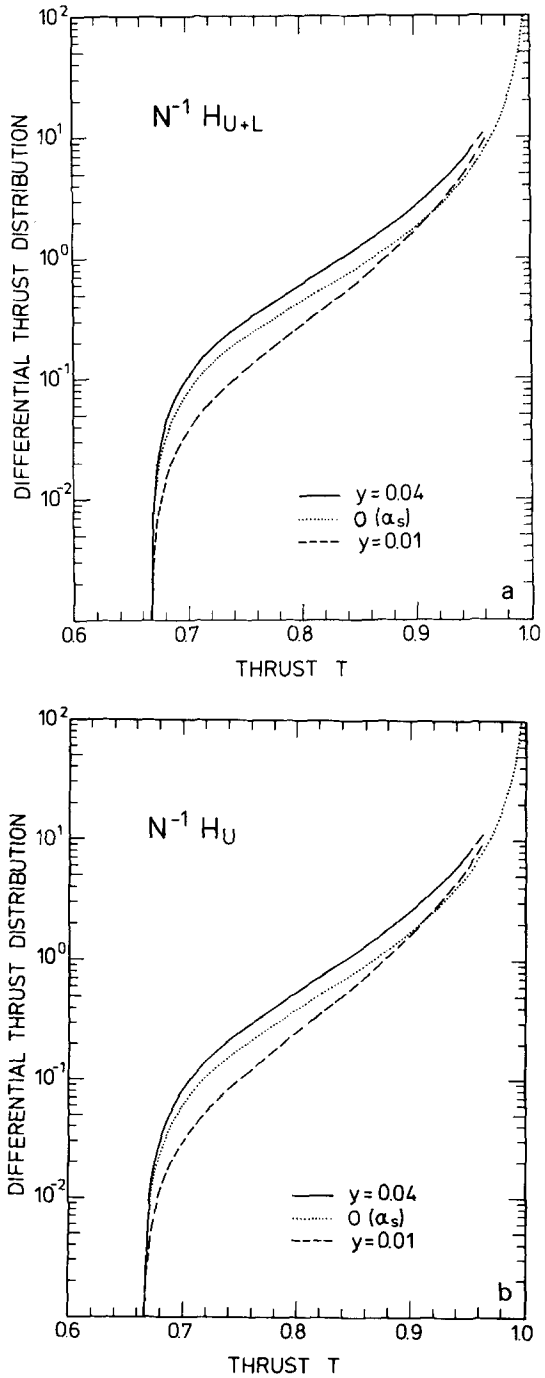

Fig. 2. $O(\alpha_s)$ and $O(\alpha_s^2)$ differential thrust distributions of helicity cross sections (a) H_{U+L}, (b) H_U, (c) H_L, (d) H_T and (e) H_I. Dotted line: $O(\alpha_s)$ result; full line: $O(\alpha_s^2)$ result ($y = 0.04$); dashed line: $O(\alpha_s^2)$ result ($y = 0.01$). Normalization factor N given in main text.

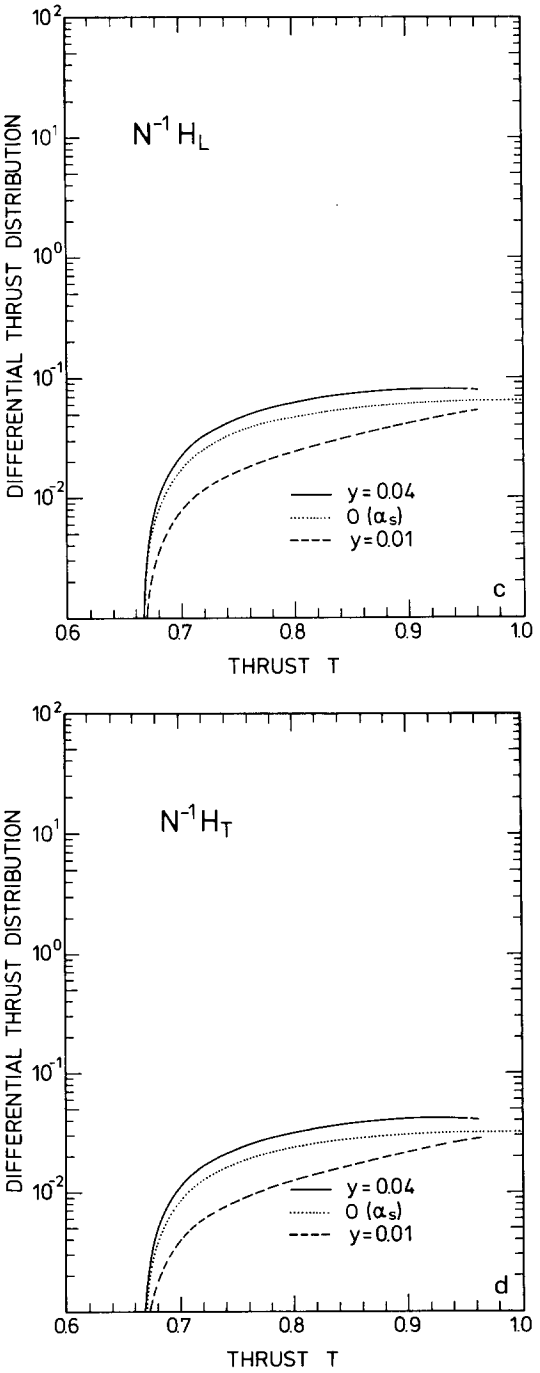

Fig. 2 (continued).

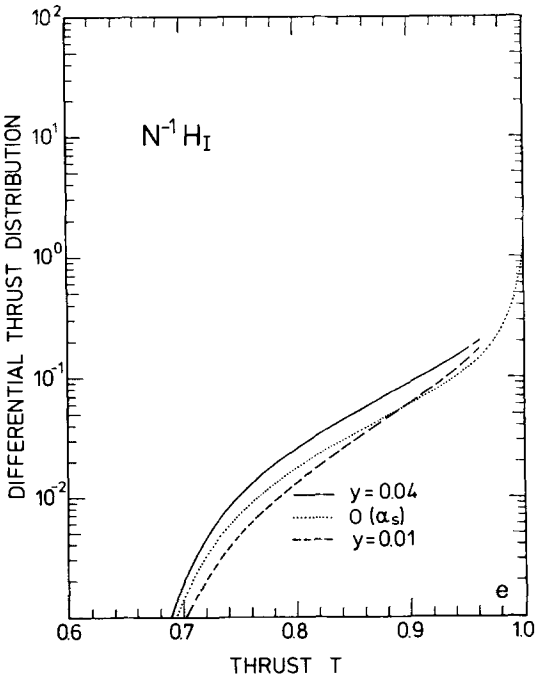

Fig. 2 (continued).

$y = 0.01$ and not much beyond $T \geqslant 0.8 - 0.85$ for $y = 0.04$. Therefore the $O(\alpha_s^2)$ curves in figs. 2 and 3 are only drawn up to thrust values $T = 0.95$. The $O(\alpha_s)$ distributions drawn in figs. 2 and 3 are of course accurate beyond $T = 0.95$ and are drawn to their singular and nonsingular limits at $T = 1$. From a practical point of view the choice $y = 0.01$ or even a smaller value of y is to be preferred since it minimizes the error of the $O(y^0)$ approximation and extends the thrust range where the analytical $O(y^0)$ results may be applied. On the other hand, this choice may be smaller than the typical hadronization scale at a given energy and may thus be unjustified from the physics point of view. In such a case one would use our analytical results for a small cut-off value $y = y_{\min}$ and fill up the phase space between $y_{\min} \leqslant y_{ij} \leqslant y_{\text{physical}}$ with Monte-Carlo generated events.

We finally remark that it would be interesting in principle to study the dependence of the $O(\alpha_s^2)$ 3-jet cross section on the resolution parameter y. However, at present energies, the experimental resolvability of jets is primarily determined by soft-hadronization effects and *not* by the invariant mass criteria of the parton pairs. Therefore it seems to be impossible to study the detailed cut-off dependence of our $O(\alpha_s^2)$ predictions at present, except possibly for the overall features of the y-dependence as indicated in figs. 2 and 3.

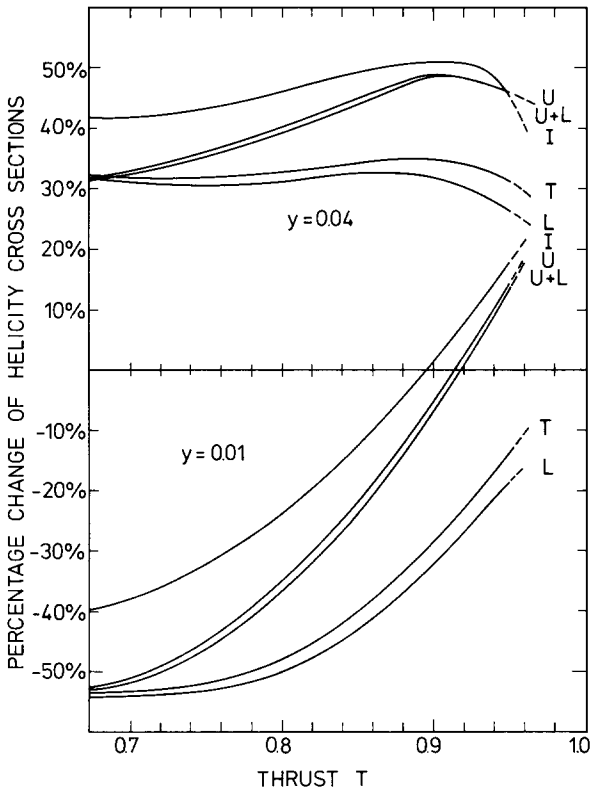

Fig. 3. Percentage change of $O(\alpha_s^2)$ differential thrust distributions relative to $O(\alpha_s)$ result for $y = 0.04$ and $y = 0.01$.

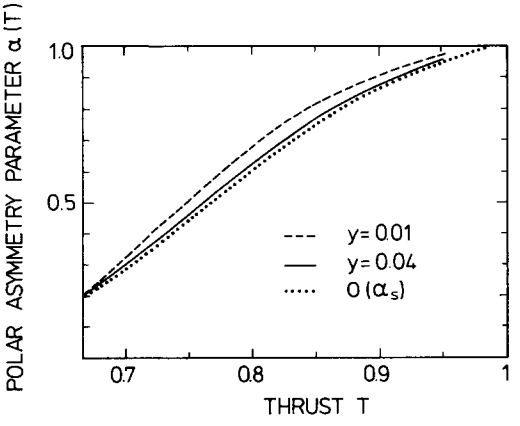

Fig. 4. Thrust dependence of asymmetry parameter $\alpha(T)$ at $O(\alpha_s)$ and $O(\alpha_s^2)$ for polar angle asymmetry of thrust axis.

6. Summary and conclusion

We have presented analytical formulas that allow one to describe the space orientation of $O(\alpha_s^2)$ 3-jet events. These formulas are simple enough to be easily incorporated into present Monte-Carlo event-generation programs. By generating oriented $O(\alpha_s^2)$ 3-jet events one could account for detector inhomogeneities when analyzing experimental data on 3-jet events. Vice versa one could check the $O(\alpha_s^2)$ QCD predictions for the orientation of 3-jet events. Using the results of this paper it is not difficult to calculate orientation effects in energy weighted cross sections or in energy–energy correlation. Results of calculating $O(\alpha_s^2)$ effects in the charge asymmetry of 3-jet production and for the gluon polarization have been given in ref. [18].

The present work completes the theoretical program of evaluating the $O(\alpha_s^2)$ corrections to oriented 3-jet events for massless quarks. The corresponding calculation for massive quarks has not yet been done so far. Although technically difficult it would be a worthwhile undertaking since it would allow one to continuously join the $O(\alpha_s^2)$ 3-jet and 4-jet regions where mass effects are routinely included.

Our results are approximate in the sense that we evaluate tree contributions to $O(y^0)$ in well-defined 3-jet regions. The additional theoretical effort necessary to include higher order y-contributions and to exactly account for the kinematic effects close to the 2-jet limit is forbidding and also not warranted since the errors of our approximations can be minimized by choosing small values for the invariant mass cut-off y.

We would like to thank A. Ali, G. Ingelman, G. Kramer, B. Lampe and T. Sjöstrand for informative discussions.

Appendix A

BEAM-POLARIZATION EFFECTS

In the presence of beam-polarization effects the 3-parton cross section formula eq. (3.1) has to be generalized to

$$d\sigma = (2\pi\alpha/q^2)^2 \Bigg[\sum_{r'=1,2,3,4} g_{r'1}(Q_f) L_{\mu\nu}^{(r')} H_{(1)}^{\mu\nu} + \sum_{r'=1,4} g_{r'4}(Q_f) L_{\mu\nu}^{(r')} H_{(4)}^{\mu\nu} \Bigg] \mathrm{dLIPS}^{(3)} \qquad (A.1)$$

The components of the electroweak coupling matrix needed in (A.1) read

$$
\begin{aligned}
g_{11} &= Q_f^2 - 2Q_f v v_f \operatorname{Re}\chi_Z + (v^2 + a^2)(v_f^2 + a_f^2)|\chi_Z|^2, \\
g_{14} &= 2Q_f v a_f \operatorname{Re}\chi_Z - (v^2 + a^2) 2 v_f a_f |\chi_Z|^2, \\
g_{21} &= Q_f^2 - 2Q_f v v_f \operatorname{Re}\chi_Z + (v^2 - a^2)(v_f^2 + a_f^2)|\chi_Z|^2, \\
g_{31} &= -2Q_f a v_f \operatorname{Im}\chi_Z, \\
g_{41} &= 2Q_f a v_f \operatorname{Re}\chi_Z - 2va(v_f^2 + a_f^2)|\chi_Z|^2, \\
g_{44} &= -2Q_f a a_f \operatorname{Re}\chi_Z + 4 v a v_f a_f |\chi_Z|^2,
\end{aligned}
\tag{A.2}
$$

where we have not yet specified the electroweak parameters v, a, v_f and a_f in terms of the Weinberg–Salam model as in sect. 2. v and a, and v_f and a_f are the electroweak vector and axial-vector coupling constants of the leptons and quarks, respectively. In the standard Weinberg–Salam model one has $v = -1 + 4\sin^2\Theta_W$ and $a = -1$ for the leptons, $v_f = 1 - \frac{8}{3}\sin^2\Theta_W$ and $a_f = 1$ for u, c, t quarks ($Q_f = \frac{2}{3}$), and $v_f = -1 + \frac{4}{3}\sin^2\Theta_W$ and $a_f = -1$ for d, s, b quarks ($Q_f = -\frac{1}{3}$). The Z_0 propagator factor χ_Z is defined in eq. (3.5).

We have written the cross section (A.1) in a form which is more general than needed for the present discussion of mass-zero quarks. The form (A.1) facilitates the inclusion of massive-quark effects which can be easily accomplished using eq. (A.1), (see ref. [13]). The lepton tensors $L_{\mu\nu}^{(r)}$ take their simplest form in the laboratory beam system ($\equiv$ overall c.m. system). We specify the laboratory beam system as follows: z-axis in e^--direction, x-axis in the accelerator plane pointing inward (along the Lorentz force). The lepton tensor has only (x, y) components in this system due to current conservation and due to the chirality-preserving vector and axial-vector current interactions. The nonvanishing components of the lepton tensor read

$$
\begin{aligned}
L_{11}^1 &= L_{22}^1 = (1 + \xi_z^- \xi_z^+), \\
L_{12}^1 &= -L_{21}^1 = -i(\xi_z^- + \xi_z^+), \\
L_{11}^2 &= -L_{22}^2 = -(\xi_x^- \xi_x^+ - \xi_y^- \xi_y^+), \\
L_{12}^2 &= L_{12}^2 = -(\xi_x^- \xi_y^+ + \xi_y^- \xi_x^+), \\
L_{11}^3 &= -L_{22}^3 = (\xi_x^- \xi_y^+ + \xi_y^- \xi_x^+), \\
L_{12}^3 &= L_{21}^3 = -(\xi_x^- \xi_x^+ - \xi_y^- \xi_y^+), \\
L_{11}^4 &= L_{22}^4 = (\xi_z^- + \xi_z^+), \\
L_{12}^4 &= -L_{21}^4 = -i(1 + \xi_z^- \xi_z^+).
\end{aligned}
\tag{A.3}
$$

The $\xi^{\pm}=(\xi_x^{\pm}, \xi_y^{\pm}, \xi_z^{\pm})$ are the polarization vectors of $e^{\pm}$ in the laboratory beam frame as specified above. Thus $\xi_x^{\pm}$ and $\xi_y^{\pm}$ denote the transverse beam polarization in and out of the accelerator plane and $\xi_3^{\pm}(\equiv \mp h^{\pm})$ the longitudinal polarization (helicity) of $e^{\pm}$. For natural transverse beam polarization of degree P one has $\xi^{\pm}=(0, \pm P, 0)$. This explicit representation of the lepton tensor can then be used to evaluate the invariant product $L_{\mu\nu}H^{\mu\nu}$ in the laboratory beam system using the $O(\alpha_s^2)$ hadron tensor components as specified in sect. 3.

Appendix B

LONGITUDINAL CROSS SECTIONS

The Lund MC requires the dynamical QCD input in terms of the helicity cross section in the (1,2)-system (q along z; $\bar{q}$ in the pos. (x, z) half plane) [10]. These can be calculated from the invariant cross sections as described in sect. 5. It turns out that a much more compact form exists for the p.c. $O(\alpha_s^2)$ results in terms of H_{U+L} and the longitudinal cross sections H_{L1}, H_{L2} and H_{L3} along q, $\bar{q}$ and g as defined in sect. 5

$$H_{Li} = H_{\mu\nu} p_i^{\mu} p_i^{\nu} / E_i^2 . \tag{B.1}$$

These scalar cross sections arise naturally in the $O(\alpha_s^2)$ 3-jet calculation when tensor integrands have to be scalarized.

The (1,2) helicity cross sections are related to H_{U+L} and the H_{Li} in the following manner

$$\begin{aligned}
H_{U1} &= H_{U+L} - H_{L1}, \\
H_{L1} &= H_{L1}, \\
H_{T1} &= \tfrac{1}{2} H_{U+L} + (1/4X)\left[\left(x_1^2 Z_1 + 2X\right) H_{L1} + x_2^2 Z_2 H_{L2} + x_3^2 Z_3 H_{L3}\right], \\
H_{I12} &= \left(-1/4\sqrt{2X}\right)\left[\left(x_2^2 - x_3^2\right) H_{L1} - x_2^2 H_{L2} + x_3^2 H_{L3}\right],
\end{aligned} \tag{B.2}$$

where Z_i and X are defined in (5.5).
For the H_{U+L} and H_{Li} one has (A = U + L, L1, L2, L3)

$$\begin{aligned}
H_A = 32\pi^2 C_F N_C B_A \frac{\alpha_s}{2\pi} \Bigg\{ 1 + \frac{\alpha_s}{2\pi} \Big[\tfrac{1}{2} N_C \left(\tilde{H}(\text{tree}) + \tilde{H}_A(\text{loop}) \right) \\
+ \left(C_F - \tfrac{1}{2} N_C \right) \left(\hat{H}(\text{tree}) + \hat{H}_A(\text{loop}) \right) + \left(\tfrac{1}{3} N_F - \tfrac{11}{6} N_C \right) H^{f}(\text{tree}) \Big] \Bigg\},
\end{aligned} \tag{B.3}$$

where the Born term functions B_A are given by

$$\begin{aligned}
B_{U+L} &= 2\left(x_1^2 + x_2^2\right)/(1 - x_1)(1 - x_2), \qquad B_{L1} = 4(1 - x_3)/x_1^2, \\
B_{L2}(1,2) &= B_{L1}(2,1), \qquad B_{L3} = 8(1 - x_3)/x_3^2 .
\end{aligned} \tag{B.4}$$

The tree-graph contributions appearing in eq. (B.3) are listed in eq. (4.4).

For the loop contributions one has ($y_{ij} = 1 - x_k$)

$$\tilde{H}_{U+L}(\text{loop}) = \tilde{g}/B_{U+L},$$

$$2\tilde{H}_{L1}(\text{loop}) = 2\tilde{H}_{L2}(\text{loop}) = 1,$$

$$\begin{aligned} 2\tilde{H}_{L3}(\text{loop}) = {} & \frac{y_{13}+y_{23}}{2y_{12}} - \frac{y_{13}^2}{2y_{12}(y_{12}+y_{13})} - \frac{y_{23}^2}{2y_{12}(y_{12}+y_{23})} \\ & + \tfrac{1}{2}\ln y_{13}\frac{y_{13}y_{23} + 2(y_{12}+y_{23})(y_{23}-y_{13})}{(y_{12}+y_{23})^2} \\ & + \tfrac{1}{2}\ln y_{23}\frac{y_{13}y_{23} + 2(y_{12}+y_{13})(y_{13}-y_{23})}{(y_{12}+y_{13})^2}, \end{aligned}$$

$$\hat{H}_{U+L}(\text{loop}) = \hat{g}/B_{U+L},$$

$$\begin{aligned} 2\hat{H}_{L1}(\text{loop}) = {} & -1 + 2\ln y_{23} + \frac{2y_{13}}{y_{13}+y_{23}} + 2\ln y_{12}\frac{y_{13}}{(y_{13}+y_{23})^2} \\ & - 2r(y_{12}, y_{13}) + 2\frac{y_{12}}{y_{13}}r(y_{12}, y_{23}), \end{aligned}$$

$$\hat{H}_{L2}(\text{loop}; 1, 2) = \hat{H}_{L1}(\text{loop}; 2, 1),$$

$$\begin{aligned} 2\hat{H}_{L3}(\text{loop}) = {} & 2\ln y_{12} + \frac{y_{13}+y_{23}}{2y_{12}} - \frac{y_{13}^2}{2y_{12}(y_{12}+y_{13})} - \frac{y_{23}^2}{2y_{12}(y_{12}+y_{23})} \\ & + \tfrac{1}{2}\ln y_{13}\frac{(2-y_{13})y_{23}}{(y_{12}+y_{23})^2} + \tfrac{1}{2}\ln y_{23}\frac{(2-y_{23})y_{13}}{(y_{12}+y_{13})^2} \\ & - r(y_{12}, y_{13}) - r(y_{12}, y_{23}), \end{aligned} \tag{B.5}$$

where $r(x, y)$ is defined in eq. (4.11) and where the functions g and $\hat{g}$ are given by

$$\begin{aligned} \tilde{g}(y_{13}, y_{23}) = {} & \ln y_{13}\left[4\frac{y_{12}+y_{13}}{y_{12}+y_{23}} - \frac{y_{13}y_{23}}{(y_{12}+y_{23})^2}\right] \\ & + \ln y_{23}\left[4\frac{y_{12}+y_{23}}{y_{12}+y_{13}} - \frac{y_{13}y_{23}}{(y_{12}+y_{13})^2}\right] \\ & + \frac{y_{12}}{y_{12}+y_{13}} + \frac{y_{12}}{y_{12}+y_{23}} + \frac{y_{12}}{y_{13}} + \frac{y_{12}}{y_{23}} + \frac{y_{13}}{y_{23}} + \frac{y_{23}}{y_{13}}, \end{aligned}$$

$$\hat{g}(y_{13}, y_{23}) = 4 \ln y_{12} \left[\frac{2y_{12}}{y_{13}+y_{23}} + \frac{y_{12}^2}{(y_{13}+y_{23})^2} \right]$$
$$+ \ln y_{13} \left[\frac{4y_{12}}{y_{12}+y_{23}} + \frac{2y_{13}}{y_{12}+y_{23}} - \frac{y_{13}y_{23}}{(y_{12}+y_{23})^2} \right]$$
$$+ \ln y_{23} \left[\frac{4y_{12}}{y_{12}+y_{13}} + \frac{2y_{23}}{y_{12}+y_{13}} - \frac{y_{13}y_{23}}{(y_{12}+y_{13})^2} \right]$$
$$- 2r(y_{12}, y_{13}) \frac{y_{12}^2 + (y_{12}+y_{23})^2}{y_{13}y_{23}} y_{13}$$
$$- 2r(y_{12}, y_{23}) \frac{y_{12}^2 + (y_{12}+y_{13})^2}{y_{13}y_{23}} + \frac{y_{12}}{y_{12}+y_{13}}$$
$$+ \frac{y_{12}}{y_{12}+y_{23}} + \frac{4y_{12}}{y_{13}+y_{23}} - \frac{y_{12}}{y_{13}} - \frac{y_{12}}{y_{23}} - \frac{y_{13}}{y_{23}} - \frac{y_{23}}{y_{13}}. \quad \text{(B.6)}$$

Since (B.6) is already contained in the present $O(\alpha_s^2)$ MC programs the inclusion of the correct $O(\alpha_s^2)$ beam-orientation and beam-polarization effects requires as an additional QCD input only the rather compact expressions (B.5).

The invariant structure functions H_i $(i = 1, \ldots 4)$ needed for the Ali et al. Monte Carlo can in fact also be calculated from the set H_{U+L}, H_{L1}, H_{L2} and H_{L3} by inverting the appropriate relations in sect. 5. One obtains

$$H_1 = -H_{U+L} - (1/4X)\left(x_1^2 Z_1 H_{L1} + x_2^2 Z_2 H_{L2} + x_3^2 Z_3 H_{L3}\right),$$

$$H_2 = \left(x_2^2/2X^2\right)\left[-2XH_{U+L} - x_1^2 Z_1 H_{L1} - \left(x_2^2 Z_2 + 2X\right) H_{L2} - x_3^2 Z_3 H_{L3}\right],$$

$$H_3 = \left(x_1^2/2X^2\right)\left[-2XH_{U+L} - \left(x_1^2 Z_1 + 2X\right) H_{L1} - x_2^2 Z_2 H_{L2} - x_3^2 Z_3 H_{L3}\right],$$

$$H_4 = (1/2X^2)\left[2Z_3 XH_{U+L} + x_1^2\left(3X + x_2^2 Z_2\right) H_{L1} + x_2^2\left(3X + x_1^2 Z_1\right) H_{L2}\right.$$
$$\left. + x_3^2\left(-3X + x_1^2 x_2^2\right) H_{L3}\right].$$

References

[1] G. Hanson et al., Phys. Rev. Lett. 35 (1975) 1609

[2] G. Kramer, G. Schierholz and J. Willrodt, Phys. Lett. B78 (1978) 249, Erratum Phys. Lett. B80 (1979) 433

[3] W. Bartel et al., JADE Collab., DESY-preprint: DESY 86-086

[4] G. Kramer and B. Lampe, Physica Scripta 28 (1983) 585

[5] G. Kramer and B. Lampe, Commun. Math. Phys. 97 (1985) 257

[6] G. Fabricius, G. Kramer, G. Schierholz and I. Schmitt, Z. Physik C11 (1982) 315

[7] R.K. Ellis, D.A. Ross and A.E. Terrano, Nucl. Phys. B178 (1981) 421
[8] J.G. Körner, G. Schuler, G. Kramer and B. Lampe, Z. Physik C32 (1986) 181
[9] A. Ali, J.G. Körner, G. Kramer, Z. Kunszt, E. Pietarinen, G. Schierholz and J. Willrodt, Nucl. Phys. B168 (1980) 409;
A. Ali, J.G. Körner, G. Kramer and J. Willrodt, Nucl. Phys. B168 (1980) 409;
A. Ali, G. Kramer, E. Pietarinen and J. Willrodt, Phys. Lett. B93 (1980) 155
[10] B. Andersson, G. Gustafson and T. Sjöstrand, Nucl. Phys. B197 (1982) 45; Phys. Rep. 97 (1983) 32
[11] J.G. Körner and G.A. Schuler, Z. Physik C26 (1985) 559
[12] T.D. Gottschalk and M.P. Shatz, Phys. Lett. B150 (1985) 451
[13] J.G. Körner and D.H. Schiller, DESY-preprint: DESY 81-043 (1981) (unpublished)
[14] J.G. Körner, G. Kramer, G. Schierholz, K. Fabricius and I. Schmitt, Phys. Lett. B94 (1980) 207
[15] H.A. Olson, P. Osland and I. Øverbo, Nucl. Phys. B171 (1980) 209
[16] E. Farhi, Phys. Rev. Lett. 39 (1977) 1587
[17] J.G. Körner, G.A. Schuler and F. Barreiro, Phys. Lett. B188 (1987) 272
[18] G.A. Schuler, Internal Report, DESY-87-1